Development 137, 745-754 (2010) doi:10.1242/dev.040238

Echinoid regulates Flamingo endocytosis to control ommatidial rotation in the *Drosophila* eye

Yu-Huei Ho[1], Mong-Ting Lien[1], Chiao-Ming Lin[1], Shu-Yi Wei[1], Li-Hsun Chang[1] and Jui-Chou Hsu[1,2,*]

SUMMARY

Planar cell polarity (PCP) refers to a second polarity axis orthogonal to the apicobasal axis in the plane of the epithelium. The molecular link between apicobasal polarity and PCP is largely unknown. During *Drosophila* eye development, differentiated photoreceptors form clusters that rotate independently of the surrounding interommatidial cells (ICs). Here, we demonstrate that both Echinoid (Ed), an adherens junction-associated cell adhesion molecule, and Flamingo (Fmi), a PCP determinant, are endocytosed via a clathrin-mediated pathway in ICs. Interestingly, we found that Ed binds the AP-2 adaptor and is required for the internalization of Fmi into ICs. Loss of *ed* led to increased amounts of Fmi on the cell membrane of non-rotating ICs and also to the misrotation of photoreceptor clusters. Importantly, overexpression of *fmi* in ICs alone was sufficient to cause misrotation of the adjacent photoreceptor clusters. Together, we propose that Ed, when internalized by AP-2, undergoes co-endocytosis with, and thereby decreases, Fmi levels on non-rotating ICs to permit correct rotation of ommatidial clusters. Thus, co-endocytosis of Ed and Fmi provides a link between apicobasal polarity and PCP.

KEY WORDS: Echinoid, Flamingo (Starry night), DE-cadherin (Shotgun), Frizzled, Planar cell polarity, Endocytosis, Cell adhesion, Adherens junction, *Drosophila*

INTRODUCTION

Epithelial cells are polarized cells with different types of cell-cell junction, including septate, gap and adherens junctions (AJs), located at different positions along the apicobasal axis. In *Drosophila*, DE-cadherin (DE-cad; Shotgun – FlyBase) and the immunoglobulin domain-containing Echinoid (Ed) are the cell adhesion molecules (CAMs) of AJs that indirectly associate with the contractile actomyosin network to mediate cell-cell adhesion (Wei et al., 2005). Cells lacking either of these two CAMs sort out from the surrounding wild-type cells (Wei et al., 2005). Interestingly, many signaling receptors, such as the Epidermal growth factor receptor (Egfr), and CAMs, such as Flamingo (Fmi; Starry night – FlyBase), are also present at AJs (see Figs 1 and 5). It has been shown that Ed blocks Egfr signaling during R8 photoreceptor selection in the *Drosophila* eye imaginal disc (Rawlins et al., 2003a; Spencer and Cagan, 2003). Fmi is an atypical cadherin that is involved in the establishment of planar cell polarity (PCP), a second polarity axis orthogonal to the apicobasal axis in the plane of the epithelium (Chae et al., 1999; Usui et al., 1999). Thus, AJs on the apicobasal axis might have additional roles to modulate PCP and various signaling pathways.

The molecular mechanism of how PCP is established in the epidermis has been extensively studied in *Drosophila*. In the *Drosophila* wing, each epithelial cell orients itself proximally to distally, with a distally pointing hair emerging from its distal vertex. Genetic analysis of this process has identified a group of core PCP genes, including *frizzled* (*fz*), *dishevelled* (*dsh*) and *fmi*, that are required for PCP establishment in a variety of tissues (Klein and Mlodzik, 2005; Mlodzik, 2002; Strutt, 2003). Fz is a seven-pass transmembrane receptor that recruits Dsh, a cytoplasmic protein, to the membrane (Axelrod et al., 1998). The *Drosophila* compound eye is another system with evident PCP. The *Drosophila* compound eye is composed of ~800 ommatidia, each containing eight photoreceptors (R1-R8) and 12 accessory cells. In third instar larvae, ommatidial assembly begins posterior to the morphogenetic furrow (MF) that sweeps across the developing disc in a posterior-to-anterior direction. The first groups of cells emerging from the MF comprise 10-15 cells and appear as an arc (row 1). When one R8 is selected from the arc cells, it recruits adjacent cells in the arc to form R2 and R5. Subsequently, R3 and R4 are recruited to complete the assembly of the ommatidial precluster (Wolff and Ready, 1993). Initially, the R3/R4 precursor pair is symmetrically arranged in the precluster. The cell closer to the equator (the dorsoventral midline) receives higher levels of Fz signaling and becomes specified as R3. Transcriptional upregulation of *Delta* in R3 then activates Notch signaling in the neighboring cell of the pair to specify it as R4 (Cooper and Bray, 1999; Fanto and Mlodzik, 1999; Tomlinson and Struhl, 1999). The photoreceptor clusters subsequently rotate 90° towards the equator (clockwise in the dorsal half and counterclockwise in the ventral half of the eye) to produce a mirror-image symmetry of ommatidia across the equator (Wolff and Ready, 1993). Loss of *fz* or other core PCP genes in the eye leads to defects in ommatidial chirality establishment (random chirality and symmetrical clusters) and rotation (Zheng et al., 1995).

Although these core PCP genes are crucial for the initial R3/R4 specification, little is known about their downstream effector genes and how they actually drive the rotation of these clusters. It has been proposed that DE-cad might integrate positive input from PCP and Egfr signaling to promote cluster rotation (Mirkovic and Mlodzik, 2006). Myosin II (Zipper) has also been proposed to generate a force within the rotating cluster during ommatidial rotation (Fiehler and Wolff, 2007). Moreover, Nemo, a serine/threonine kinase, is required in a subset of photoreceptors to regulate the speed of

[1]Institute of Molecular Medicine, Department of Life Science, National Tsing Hua University, Hsinchu, Taiwan 30034, Republic of China. [2]Department of Biological Science and Technology, National Chiao Tung University, Hsinchu, Taiwan 30034, Republic of China.

*Author for correspondence (lshsu@life.nthu.edu.tw)

Accepted 7 January 2010

rotation (Fiehler and Wolff, 2008). Thus, most studies suggest roles for these effector genes in the rotating clusters; however, it remains largely unknown whether the non-rotating interommatidial cells (ICs) might also regulate the rotation of the adjacent photoreceptor clusters.

Both Ed and Fmi have been shown to be present in the endocytic compartment, indicating that they are endocytosed (Rawlins et al., 2003b; Rawls and Wolff, 2003; Strutt and Strutt, 2008). During endocytosis, adaptors, such as the AP-2 complex, function to specifically recognize cargo receptors and to stimulate clathrin assembly (Robinson, 2004). Currently, it is unclear whether Ed and Fmi are internalized via the same mechanism. Here, we demonstrate that Ed is expressed uniformly in the ICs but is downregulated in the photoreceptor cluster. This is in contrast to Fmi, which is detected at lower levels in the ICs but is enriched at R3/R4/R8 photoreceptors (Das et al., 2002; Strutt et al., 2002). Ed binds the AP-2 adaptor and positively regulates the endocytosis of Fmi on ICs. Interestingly, loss of *ed* leads to misrotation of photoreceptor clusters and to accumulation of Fmi on the plasma membrane of the non-rotating ICs. As overexpression of Fmi in ICs alone is sufficient to cause misrotation of the photoreceptor clusters, we propose that Ed, when internalized, is co-endocytosed with Fmi and thereby downregulates Fmi levels on the non-rotating ICs to allow correct ommatidial rotation. Thus, co-endocytosis of Ed and Fmi provides a link between apicobasal polarity and PCP.

MATERIALS AND METHODS

Drosophila genetics

The following stocks were used: ed^{lx5} (Bai et al., 2001), fmi^{E59} (Usui et al., 1999), $ft^{G\text{-}rv}$ (Mahoney et al., 1991), ds^{UA071} (Adler et al., 1998), $sty^{\Delta 55}$ (Hacohen et al., 1998), $Rab5^{2}$ (Wucherpfennig et al., 2003), Hrs^{D28} (Littleton and Bellen, 1994), *UAS-shi*^{ts} (Waddell et al., 2000), *GMR-Gal4* (Freeman, 1996), *tubulin-Gal4* (Bloomington Stock Center), *tubulin-Gal80*^{ts} (Bloomington Stock Center), *UAS-α-Adaptin-RNAi* [Vienna *Drosophila* RNAi Center (VDRC)], *UAS-Clathrin heavy chain-RNAi* (VDRC), *UAS-ed-RNAi* (VDRC), *UAS-fz-RNAi* (Bastock and Strutt, 2007), *UAS-dsh-RNAi* (Bastock and Strutt, 2007), *UAS-Rab5-RNAi* (VDRC), *UAS-Rab7-GFP* (Entchev et al., 2000), *UAS-Fmi-EYFP* (Kimura et al., 2006), *UAS-ed* (Bai et al., 2001), *UAS-Ed*$^{\Delta intra}$ (Bai et al., 2001), *UAS-Ed*^{intra}-GFP (Lin et al., 2007), *UAS-fmi* (Usui et al., 1999), *UAS-DE-cad* (Sanson et al., 1996), *ubi-P63E-shg-GFP* (Oda and Tsukita, 2001) and *mδ0.5-lacZ* (Cooper and Bray, 1999).

To ubiquitously overexpress *ed-RNAi* throughout the whole eye disc, we first generated a *tubulin-Gal4,tubulin-Gal80*^{ts} recombinant (referred to as *tub-Gal80*^{ts}*-Gal4*) and then used it to drive *ed-RNAi* expression at restrictive temperature (29°C) for 2-3 days before dissection. Loss-of-function mosaic clones were generated using *eyFLP*-induced mitotic recombination and marked with *ubi-GFP* (Newsome et al., 2000). Flip-out clones overexpressing various transgenes (including *UAS-RNAi*) were generated by *P[act5C>y+>Gal4] P[UAS-GFP.S65T]/CyO* (Ito et al., 1997). Entirely ed^{lx5} mutant eyes were generated using the EGUF (*eyeless*-Gal4 UAS-FLP) system of recombination (Stowers and Schwarz, 1999).

Live imaging, immunohistochemistry and histology

For immunostaining, third instar larval eye imaginal discs were dissected, fixed and then processed as described (Islam et al., 2003). For live imaging, third instar larval eye discs were dissected and placed in a drop of serum-free M3 medium with or without 200 μM chloroquine (Sigma) at room temperature for 4 hours. The tissue explants were then washed in serum-free M3 and processed for immunostaining. Antibodies used were: rat anti-Ed (Wei et al., 2005), mouse anti-Fmi [1:20; Developmental Studies Hybridoma Bank (DSHB)], rabbit anti-Fz (1:300) (Bastock and Strutt, 2007), rat anti-Dsh (1:1000) (Strutt et al., 2006), mouse anti-Egfr (1:50) (Chang et al., 2008), rat anti-DE-cad (DCAD2; 1:20; DSHB), mouse anti-Arm (N2-7A1, 1:40; DSHB), mouse anti-Discs large (1:1000; DSHB), rat anti-Elav (1:500; DSHB). Alexa Fluor 594-phalloidin, which binds to F-actin (Invitrogen), and Cy3- and Cy5-conjugated secondary IgGs (Jackson ImmunoResearch) were used. Fluorescent images were obtained using a Zeiss 510 confocal microscope. Adult eye sections and eyes containing homozygous mutant clones were prepared and analyzed as described (Bai et al., 2001).

Quantification

The numbers of Fmi-EYFP punctate dots, of Rab7-GFP and Fmi colocalized particles and of Rab7-GFP and Egfr colocalized particles were quantified manually for individual *z*-sections, using the same threshold and equivalent areas for the wild-type and mutant tissues. The numbers of punctate dots were then averaged for each genotype.

Protein interaction assays

For GST pull-down assays, 15 μg purified GST-Ed^{intra} proteins was incubated with in vitro-translated ^{35}S-labeled AP-50 protein (Promega TNT System) as described (Lin et al., 2007).

Quantitative PCR

Total RNA was extracted from eye imaginal discs with Trizol (Invitrogen) and cDNA synthesized with the Cells-to-cDNA System (Ambion). Aliquots equivalent to 0.4% of the product were used as template in a quantitative PCR reaction using the SYBR Green Kit (Applied Biosystems). α*Tub84B* was used for normalization. Three independent experiments were averaged.

RESULTS

Dynamic expression of Ed during ommatidial rotation

We analyzed the expression pattern of Ed in the eye disc epithelium using an antibody against its intracellular domain. The specificity of this antibody has been confirmed by immunoblot analysis and by the lack of immunostaining within *ed* mutant clones in both eye and wing discs (Lin et al., 2007; Wei et al., 2005). Ed was uniformly distributed on the AJs in all cells anterior to, and within, the MF (Fig. 1A). Posterior to the MF, Ed remained uniform in the ICs but was greatly downregulated in the R8/R2/R5 and, to a lesser extent, in the R3/R4 cells of the ommatidial precluster from row 2 (Fig. 1A-C). This expression pattern, with high levels of Ed in the ICs but low levels in the photoreceptor cluster, was largely complementary to that of Fmi, which accumulated at low levels in the ICs but was enriched at R3/R4 and R8 of the photoreceptor cluster and subsequently only at R4 (Fig. 1A,C). Thus, for photoreceptor clusters in rows 4-6, very low levels of Ed were detected at the interface between R8/R2/R5 and the adjacent ICs, whereas slightly higher levels of Ed were detected at the interface between R3/R4 and the adjacent ICs (Fig. 1C). By contrast, Fmi was enriched to high levels at the interface between R8 and the two to three contacting ICs, whereas variable amounts of Fmi accumulated at the interface between R3/R4 and the five to seven contacting ICs (Fig. 1C; see below).

Similarly, the *ed* expression pattern was also largely complementary to that of *ubi-P63E-shg-GFP*, which was enriched at the junctional interface of photoreceptor clusters (Fig. 1C). The expression pattern of *ubi-P63E-shg-GFP* is the sum of DE-cad and Cadherin-N (DN-cad) (Fig. 1A‴) (Mirkovic and Mlodzik, 2006). Thus, the complementary expression pattern seen with Ed (high levels in the ICs but low levels in the cluster) and DE-cad/DN-cad (enrichment in the cluster), together with the presence of low levels of Ed at the interface between photoreceptor clusters and ICs, partially resembled the cell sorting seen between Ed-expressing and Ed-non-expressing cells of *ed* mutant clones in the wing disc (Wei et al., 2005); such Ed-non-expressing cells accumulate high levels of DE-cad and Armadillo (Arm) and do not form proper AJs with the surrounding Ed-expressing cells (Wei et al., 2005).

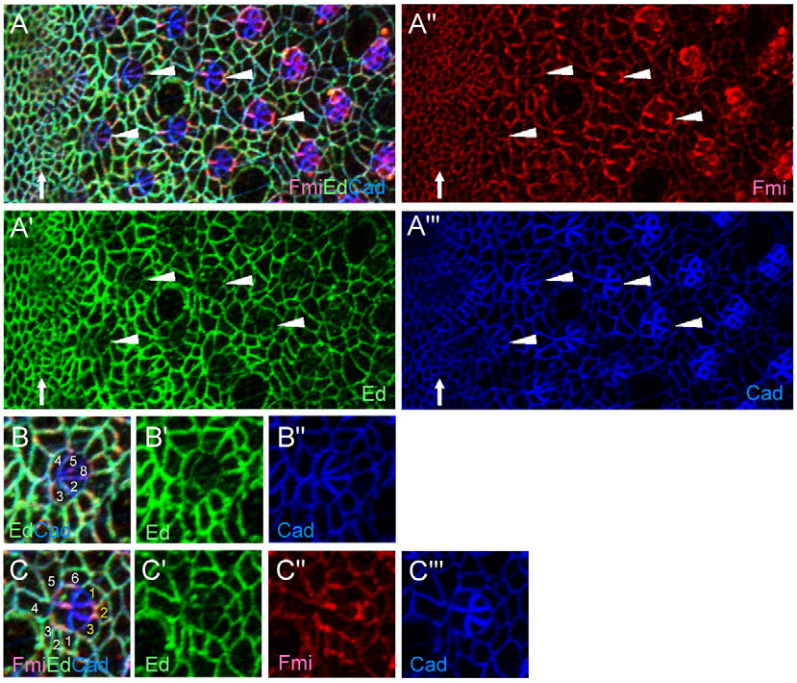

Fig. 1. Dynamic distribution of Ed during ommatidial rotation. (**A-A‴**) Dynamic distribution of Ed (green), Fmi (red) and *ubi-P63E-shg-GFP* (blue) in *Drosophila* third instar larval eye imaginal discs. Ed is present in all cells of the eye disc (labeled by *ubi-P63E-shg-GFP*) but is detected at much lower levels in the photoreceptors of the ommatidial precluster from row 2 (arrowheads). The expression pattern of *ubi-P63E-shg-GFP* is the sum of that of DE-cad and DN-cad. Arrow indicates the morphogenetic furrow (MF). (**B-B‴**) High magnification of preclusters in row 3 labeled for Ed (green), Fmi (red) and *ubi-P63E-shg-GFP* (blue). The photoreceptors of this precluster are numbered. (**C-C‴**) High magnification of preclusters in row 5 labeled for Ed (green), Fmi (red) and *ubi-P63E-shg-GFP* (blue). The ICs bordering the apposed R3/R4 cells are numbered in white, those bordering the apposed R8 cell in yellow.

Accumulation of Ed and Fmi in the ICs is regulated by endocytosis

The AP-2 complex is composed of α/α-Adaptin, β2, μ2 (AP-50) and σ2 subunits and acts as an adaptor between cargo receptors and clathrin-coated vesicles during endocytosis (Robinson, 2004). The intracellular domain of Ed (Ed^{intra}) includes five copies of the protein-sorting signal YXXΦ (where Φ is a bulky hydrophobic amino acid), which could potentially interact with the AP-50 subunit of the AP-2 complex (Robinson, 2004). GST pull-down assays were used to test whether Ed can directly interact with AP-50 and act as a specific cargo of AP-2. Interestingly, we found that Ed^{intra} bound to in vitro-translated AP-50 (Fig. 2A).

Next, we asked whether Ed is internalized and degraded via clathrin- and dynamin-mediated endocytosis. To test this, we first examined the effects of AP-2 and clathrin on Ed levels by generating ectopic RNAi clones to deplete α-*Adaptin* and *Clathrin heavy chain* expression in the eye imaginal discs. Interestingly, plasma membrane-associated Ed levels were upregulated in the ICs (Fig. 2B and data not shown), but not in the photoreceptor cluster, which still had very low levels of Ed (Fig. 2B, inset). Thus, clathrin-dependent endocytosis plays a crucial role in the regulation of Ed levels in ICs, but a minor role, if any, in the regulation of Ed levels in the cluster.

Second, we examined the effects of *shibire* (*shi*) and *Rab5* on Ed levels by generating ectopic clones overexpressing the temperature-sensitive shi^{ts} transgene and $Rab5^{2}$ mutant clones. Both the dynamin ortholog Shi and the GTPase Rab5 regulate cargo entry into the early endosome (Chen et al., 1991; Seto et al., 2002; van der Bliek and Meyerowitz, 1991). Strikingly, Ed levels were greatly elevated on the plasma membrane of shi^{ts}-overexpressing ICs at restrictive (29°C) temperatures (Fig. 2D), but Ed formed large punctate structures in $Rab5^{2}$ mutant ICs (Fig. 2F). By contrast, Ed levels were not upregulated in the photoreceptor cluster in shi^{ts}-overexpressing and *Rab5-RNAi*-overexpressing clones, which still had very low levels of Ed (see Fig. S1 in the supplementary material, arrowheads). The accumulation of lower levels of Ed on ICs in both α-*Adaptin* and *Clathrin heavy chain* RNAi clones compared with $Rab5^{2}$ null mutant clones might reflect only partial silencing of these two genes or, alternatively, the involvement of other clathrin-independent endocytic pathways.

Third, we examined Ed levels in cells mutant for *Hepatocyte growth factor-regulated tyrosine kinase substrate* (*Hrs*). Hrs mediates the recruitment of ubiquitylated cargo in the early endosome (Hicke and Dunn, 2003; Seto et al., 2002). In Hrs^{D28} mutant clones, Ed appeared as punctate dots, reminiscent of vesicle staining, in the ICs (Fig. 2G).

Finally, we used the drug chloroquine to block lysosome function in tissue explants and observed Ed as punctate dots in the interommatidial lattice (Fig. 2I,J). Altogether, our results strongly suggest that Ed is internalized and degraded via clathrin- and AP-2-mediated endocytosis in the non-rotating ICs.

Fmi is known to be present in the endocytic compartment of R3/R4 photoreceptors and wing disc epithelial cells (Rawls and Wolff, 2003; Strutt and Strutt, 2008). Although Fmi does not possess a sorting signal for the AP-2 adaptor, we suggest, based on the following results, that Fmi levels in ICs, as with Ed, are regulated by clathrin-dependent endocytosis. First, levels of membrane-associated Fmi in ICs increased when α-*Adaptin* was silenced by RNAi (Fig. 2C). Second, Fmi levels were greatly elevated on the plasma membrane of shi^{ts}-overexpressing cells at restrictive temperature (Fig. 2E) and Fmi colocalized with Ed in large puncta in $Rab5^{2}$ mutant cells (Fig. 2F). Third, Fmi colocalized with Ed as small puncta in Hrs^{D28} mutant cells (Fig. 2G) or when lysosome function was blocked by chloroquine in tissue explants (Fig. 2J). Finally, both Ed and Fmi colocalized with the late endosomal marker Rab7 (Fig. 2H). Thus, Ed and Fmi are trafficked via the same endocytic route in ICs.

Ed regulates the levels of Fmi in the ICs

Although Ed and Fmi are endocytosed by the clathrin- and dynamin-dependent pathway, Ed accumulated at higher levels in ICs than Fmi (Fig. 1A). A simple explanation for this discrepancy is that Ed and Fmi are internalized and/or synthesized at different rates. Unexpectedly, we found that in ed^{lx5} mutant clones, high levels of

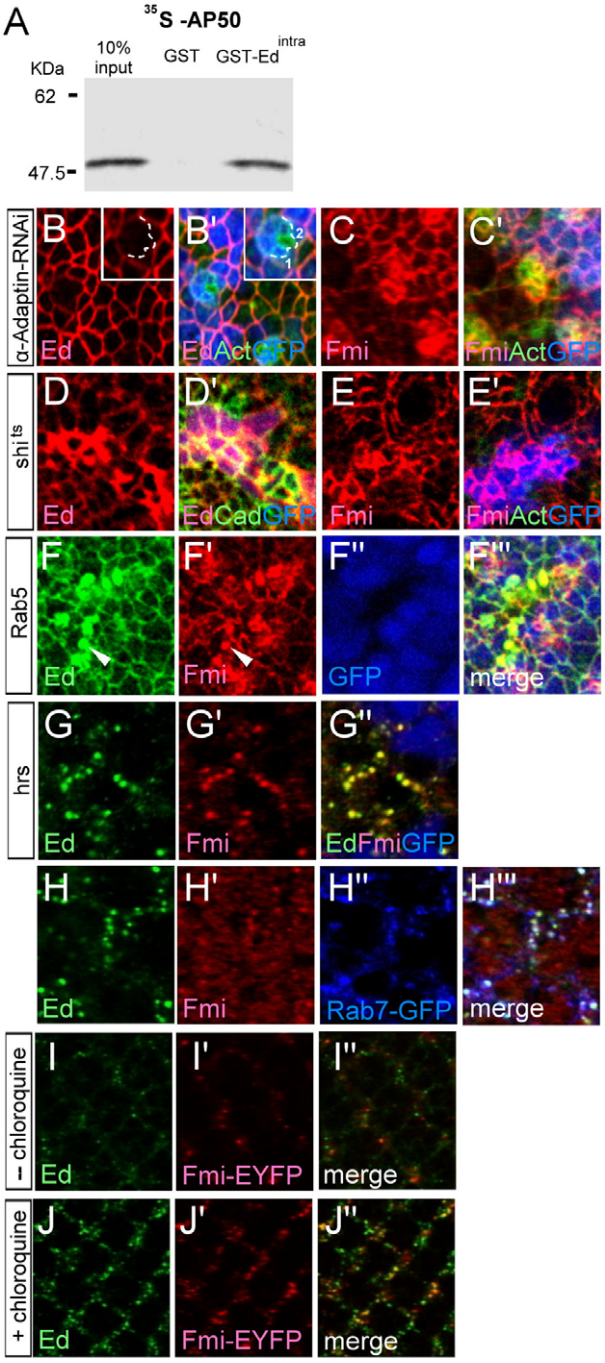

Fig. 2. Accumulation of Ed and Fmi in the ICs is regulated by endocytosis. (**A**) In vitro binding of ^{35}S-labeled AP-50 to GST-Ed^{intra}. (**B-C′**) α-*Adaptin-RNAi* clones labeled for Ed (red in B), Fmi (red in C), GFP (blue) and actin (green). (Inset) Higher magnification shows that levels of Ed in the photoreceptor cluster are not increased. Dashed lines indicate the Ed-free interface between R8/R2/R5 and the two adjacent ICs (numbered). (**D-E′**) *shi^{ts}* ectopic clones labeled for Ed (red in D), Fmi (red in E), DE-cad (green in D), actin (green in E) and GFP (blue). (**F-F‴**) *Rab5^{2}* mutant clones labeled for Ed (green), Fmi (red) and GFP (blue). Loss of GFP indicates mutant tissue. Arrowhead indicates Ed (F) and Fmi (F′) in large puncta. (**G-G″**) *Hrs^{D28}* mutant clone labeled for Ed (green), Fmi (red) and GFP (blue). Loss of GFP marks mutant tissue. (**H-H‴**) Colocalization of Ed (green in I), Fmi (red in I′) and Rab7-GFP (blue in I″) in wild-type disc. (**I-J″**) Colocalization of Ed (green) and Fmi-EYFP (red) particles in the subapical region of wild-type disc explants without (I) and with (J) chloroquine treatment.

Fmi accumulated at the plasma membrane of ICs, comparable to the enrichment of Fmi bordering R3 and R4 (Fig. 3A). Similar results were obtained in *ed-RNAi* clones (data not shown). However, both the levels and distribution pattern of Fmi in the photoreceptor cluster (enrichment of Fmi at the R3/R4 border and the later accumulation in R4) were largely unaltered within the *ed* mutant clones (Fig. 3A, arrowheads). Thus, *ed* regulates the levels of Fmi only in ICs and not in photoreceptor clusters.

As shown above, for the ommatidial clusters at rows 4-6 of the wild-type discs, it required five to seven ICs to border the apposed R3/R4 cells (Fig. 1C). We further found that 19.2%, 51.3% and 29.5% of ommatidia (n=78) used five, six and seven ICs, respectively, to border the apposed R3/R4 cells. By contrast, when *ed-RNAi* was ubiquitously overexpressed in the whole eye disc using the *tub-Gal80^{ts}-Gal4* system (see Materials and methods), just four to six Fmi-upregulating ICs were sufficient to cover the border with R3/R4 cells (compare Fig. 3B with 3C), and 27.7%, 43.1% and 29.2% of ommatidia (n=202) used four, five and six ICs, respectively, to border the apposed R3/R4 cells. The requirement for fewer ICs to contact R3/R4 when *ed* was knocked down indicated that each Fmi-upregulating IC, on average, contacted the R3/R4 cells with a longer adhesion interface. As shown in Fig. 3C, the R4 cell was almost covered by the IC4 only. It has been shown that the interface length between cells is correlated with the strength of adhesion (Hayashi and Carthew, 2004). Thus, our result is consistent with the possibility that these Fmi-upregulating ICs adhered more strongly with the Fmi-expressing R3/R4 cells.

Notably, in both *ed* mutant clones and *ed-RNAi* clones, not only was Fmi upregulated in the apical junctions of ICs, but Fz and Dsh were also upregulated in the ICs (Fig. 3D and data not shown). Similar to Fmi, the enrichment of Fz at R3/R4 borders and the later accumulation in R4 in the photoreceptor cluster were largely unaffected by the elevated Fmi/Fz levels in the ICs (Fig. 3D, arrowheads). This suggests that R3/R4 fate specification is largely normal in *ed* mutant clones. It was previously shown that Fmi, when overexpressed, recruits Fz and Dsh to apical junctions in the pupal wing (Strutt and Strutt, 2008). To confirm that the higher levels of Fz/Dsh in the ICs are indeed recruited by the upregulated Fmi, we generated ectopic clones overexpressing both *ed-RNAi* and *fmi-RNAi*. As expected, Fz and Dsh were no longer detectable at the apical junctions in the double-RNAi clones (data not shown). This result indicates that in ICs, the upregulated Fmi recruited Fz and Dsh to AJs. Consistent with this, Fz shared a similar distribution pattern with Fmi in both wild-type and *tub-Gal80^{ts}-Gal4>ed-RNAi* discs (see Fig. S2 in the supplementary material). To test whether *fmi* might also regulate the levels of Ed, we performed the opposite experiment, by generating *fmi^{E59}* clones, but Ed levels were not affected (Fig. 3E).

As Ed is a CAM, we first asked whether other CAMs might have a similar effect on Fmi levels. For this, we looked at the atypical cadherins Fat and Dachsous (Ds), which are both upstream regulators of PCP signaling (Yang et al., 2002). We generated *fat* and *ds* mutant clones in the eye discs and found that Fmi levels were not altered in the ICs in either case (see Fig. S3A,B in the supplementary material). This result indicates that the effect on Fmi levels is *ed* specific.

Ed negatively regulates the EGF signaling pathway and EGF signaling regulates ommatidial rotation (Brown and Freeman, 2003; Gaengel and Mlodzik, 2003; Strutt and Strutt, 2003). We then asked whether other negative regulators of EGF signaling, such as *argos* (*aos*) and *sprouty* (*sty*), also upregulated Fmi levels in ICs. To this end, we generated *sty$^{\Delta 55}$* mutant clones in the eye discs and found

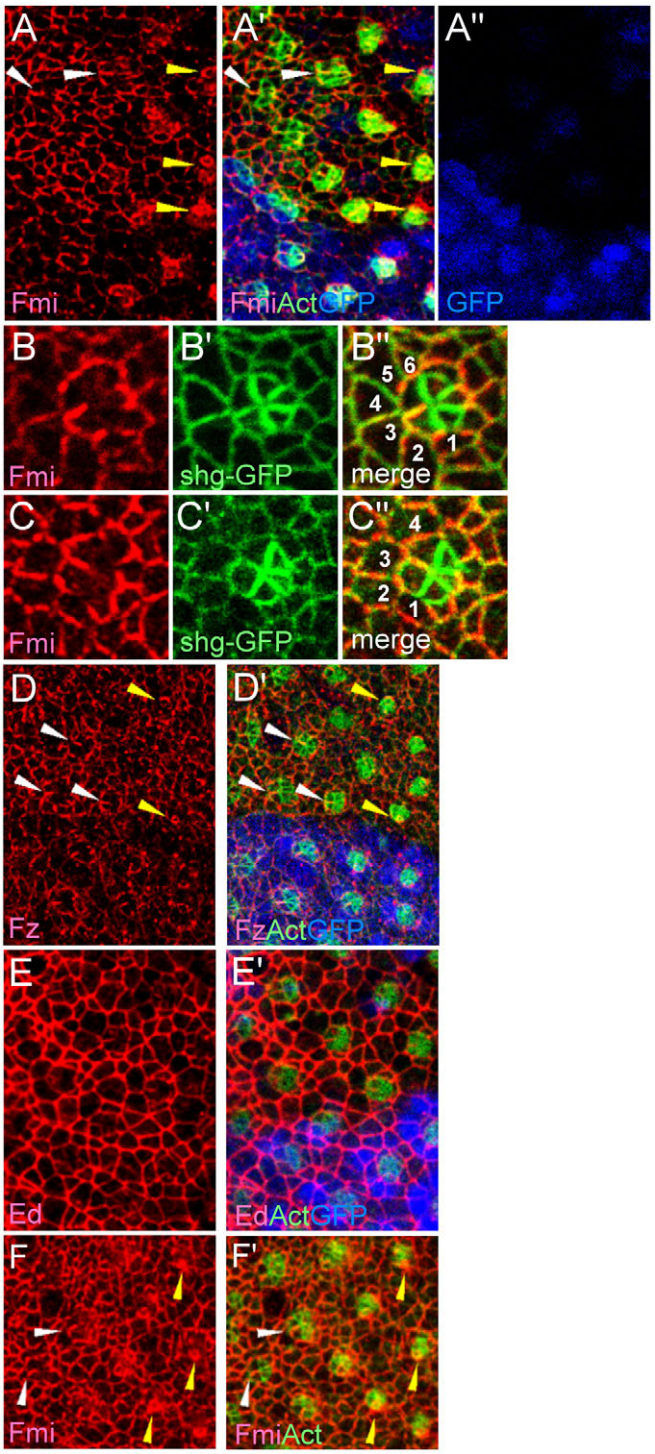

Fig. 3. Ed regulates Fmi levels in the ICs. (**A-A″**) ed^{1x5} mutant clones labeled for Fmi (red), actin (green) and clones marked by loss of GFP (blue). Both the enrichment of Fmi at the R3/R4 border (white arrowheads) and the asymmetric accumulation in R4 (yellow arrowheads) are unaltered. (**B-C″**) High magnification of preclusters at row 4 in wild-type (B) and *tub-Gal80^{ts}-Gal4>ed-RNAi* (C) discs labeled for Fmi (red) and *ubi-P63E-shg-GFP* (green). There are six (B) and four (C) ICs (numbered) bordering the apposed R3/R4 cells. (**D**,**D′**) ed^{1x5} mutant clones labeled for Fz (red), actin (green) and GFP (blue). Both the enrichment of Fz at the R3/R4 border (white arrowheads) and the asymmetric accumulation in R4 (yellow arrowheads) are unaltered. (**E**,**E′**) fmi^{E59} clone labeled for Ed (red), actin (green) and GFP (blue). (**F**,**F′**) Entirely ed^{1x5} mutant eye discs labeled for Fmi (red) and actin (green). Both the enrichment of Fmi at the R3/R4 border (white arrowheads) and the asymmetric accumulation in R4 (yellow arrowheads) are unaltered.

that Fmi was not upregulated in ICs (see Fig. S3C in the supplementary material). Similarly, we found that Fmi was not upregulated in ICs in $aos^{\Delta 7}$ mutant clones (data not shown), consistent with previous reports (Gaengel and Mlodzik, 2003; Strutt and Strutt, 2003).

Finally, *ed* mutant cells within the small ed^{1x5} clones adopt apical constrictions and sort out from the wild-type cells in the wing discs (Wei et al., 2005). However, *ed* mutant cells within larger ed^{1x5} clones have an apical surface that is similar to that of the wild-type cells (Wei et al., 2005). To exclude the possibility that the increased density of Fmi staining was due to the reduced apical surface in the *ed* mutant cells, we generated entirely ed^{1x5} mutant eye discs (Stowers and Schwarz, 1999) or ubiquitously overexpressed *ed-RNAi* in the whole eye disc, using the *tub-Gal80^{ts}-Gal4* system, to prevent apical constriction and cell sorting. Fmi levels in ICs were still upregulated (Fig. 3F and data not shown).

Altogether, these data suggest that Ed specifically regulates the levels of Fmi in ICs and that this effect is not mediated through Egfr signaling or through reduced apical surface area.

Ed regulates the endocytosis of Fmi in the ICs

To explore the mechanism of Ed regulation of Fmi levels, we first asked whether *ed* affects the transcription of *fmi*. In situ hybridization of *fmi* did not reveal any difference in *fmi* expression between wild-type and entirely ed^{1x5} mutant eye discs (data not shown). To confirm this, we compared the levels of *fmi* mRNA in imaginal discs in wild-type and entirely ed^{1x5} mutant eye discs by quantitative PCR. Lower *fmi* mRNA levels were in fact found in the ed^{1x5} mutant discs (Fig. 4A), indicating that the elevation of Fmi levels by *ed* is probably at the post-transcriptional level. Given that both Ed and Fmi localized to AJs and were internalized via a similar clathrin-dependent process, we hypothesized that Ed, being a cargo of AP-2, when endocytosed, might facilitate Fmi endocytosis. This mechanism of co-endocytosis can be achieved directly by association between Ed and Fmi at AJs and/or indirectly via the bystander effect, as Ed and Fmi are distributed uniformly at AJs.

To test our co-endocytosis model, we first asked whether loss of *ed* would interfere with the endocytosis of Fmi. Indeed, we observed that in *tub-Gal80^{ts}-Gal4>ed-RNAi* discs, Fmi was upregulated at apical surfaces (compare Fig. 4B with 4D), but the numbers of Fmi and Rab7-GFP colocalized particles were significantly reduced compared with wild-type discs (compare Fig. 4C with 4E; Fig. 4F). Similarly, the numbers of internalized Fmi-EYFP particles were also significantly reduced in *tub-Gal80^{ts}-Gal4>ed-RNAi* discs compared with wild-type discs (Fig. 4G). Thus, in the absence of Ed, Fmi is endocytosed at a slower rate, which, in turn, might be responsible for the accumulation of Fmi on the membrane.

Second, our model would predict a requirement for the sorting signal in Ed^{intra} to promote co-endocytosis. To verify this, we used *GMR-Gal4* to express either *UAS-ed*, *UAS-Ed$^{\Delta intra}$* (which contains the transmembrane and extracellular domains but lacks the intracellular domain and therefore all of the sorting signal) or *UAS-Ed^{intra}*-GFP (which contains the transmembrane and intracellular domains) in ed^{1x5} mutant clones (Bai et al., 2001). Interestingly, only

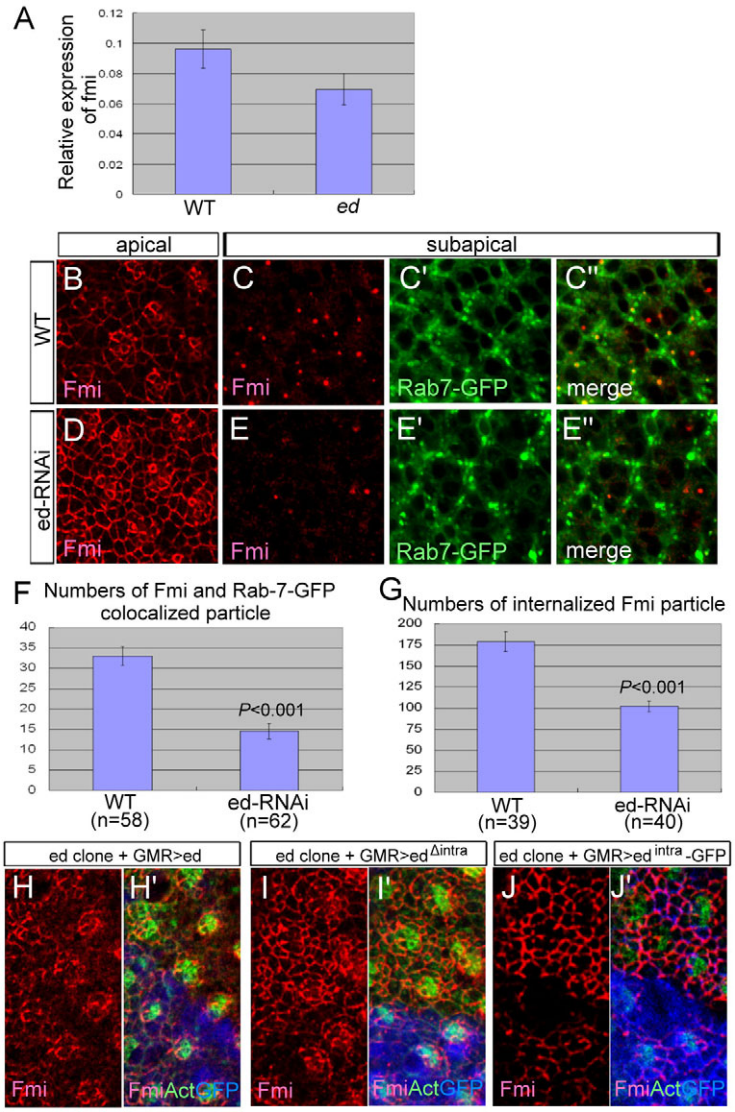

Fig. 4. Ed regulates the endocytosis of Fmi in the ICs. (**A**) Quantitation of *fmi* mRNA levels in wild-type and entirely ed^{1x5} mutant eye discs. Bars indicate mean ± s.d. (**B-E″**) Colocalization of Fmi and Rab7. (B,D) Fmi (red) levels at the apical region of wild-type (B) and *tub-Gal80^{ts}-Gal4>ed-RNAi* (D) discs. (C,E) Colocalization of internalized Fmi (red) and Rab7-GFP (green) at subapical region of wild-type (C) and *tub-Gal80^{ts}-Gal4>ed-RNAi* (E) discs. (**F**) Quantitation of internalized Fmi-EYFP particles in wild-type and *tub-Gal80^{ts}-Gal4>ed-RNAi* discs. Bars indicate mean ± s.e.m. (**G**) Quantitation of internalized Fmi and Rab7-GFP colocalized particles in wild-type and *tub-Gal80^{ts}-Gal4>ed-RNAi* discs. Bars indicate mean ± s.e.m. (**H-J'**) The expression of full-length Ed (H), but not of $Ed^{\Delta intra}$ (I) and Ed^{intra}-GFP (J), by *GMR-Gal4* rescues the upregulation of Fmi (red) levels in the ed^{1x5} mutant clones (lack of *ubi-nls-GFP*). Photoreceptor clusters are labeled for actin (green).

the full-length Ed, but not $Ed^{\Delta intra}$, could rescue the upregulation of Fmi in the ed^{1x5} mutant clones, indicating that the intracellular domain of Ed with the sorting signal is required in this process (Fig. 4H,I). Surprisingly, Ed^{intra} (with all sorting signals) alone did not rescue the upregulation of Fmi in the ed^{1x5} mutant clones (Fig. 4J), indicating that both the extracellular domain (for homophilic interaction) and the intracellular domain (with the sorting signals) of Ed were required in this process.

Third, we asked at which step *ed* might operate to regulate Fmi endocytosis. We demonstrated accumulation of Fmi at the plasma membrane in ed^{1x5} mutant clones (Fig. 3A). This was similar to the accumulation pattern detected in α-*Adaptin-RNAi* clones and ectopic shi^{ts} clones (Fig. 2C,E), but unlike the punctate pattern detected in $Rab5^{2}$ and Hrs^{D28} mutant clones (Fig. 2F,G). Thus, *ed* regulates Fmi endocytosis at a step before the action of *Rab5*/*Hrs*.

Finally, we asked whether Ed positively regulates the endocytosis of Fmi directly via molecular interaction or indirectly. We answered this question with an in vivo co-immunoprecipitation experiment in *tub>fmi-EYFP* embryos. However, we failed to detect any Ed co-precipitated with Fmi-EYFP or, in the converse experiment, any co-immunoprecipitation of Fmi-EYFP with Ed (data not shown). Thus, there is no evidence that Ed directly binds Fmi.

Ed regulates the endocytosis of Egfr

To determine whether *ed* affects receptors/CAMs other than Fmi, we examined the levels of Egfr, DE-cad and Discs large (Dlg; Dlg1 – FlyBase) in ed^{1x5} mutant clones. Egfr and Arm have overlapping distributions at AJs (Fig. 5B), whereas Dlg is a CAM at septate junctions. In wild-type tissue (lower part of Fig. 5A), Egfr was detected at low levels in cells within the MF, the emerging arc cells (Fig. 5A, white arrow) and in cells of developing ommatidia up to one to two rows posterior to the MF (Fig. 5A, yellow arrow), but was barely detectable in more posterior cells (Fig. 5A). Intriguingly, in ed^{1x5} mutant clones covering the MF, membrane-associated Egfr was moderately upregulated relative to their wild-type neighbors (upper part of Fig. 5A) and two R8 cells, instead of one, were selected from a larger group of arc cells with upregulated Egfr (Fig. 5B, arrowheads). Raised Egfr levels were also detected in the more posterior cells if the detector gain of the confocal microscope was increased (Fig. 5C). Similarly, DE-cad was also elevated, although to a lesser extent (Fig. 5D). By contrast, the level of Dlg was not affected (Fig. 5E), indicating that Ed specifically affects molecules at AJs. To confirm that the upregulation of Egfr on the membrane is also regulated by Ed-mediated endocytosis, we asked whether loss of *ed* would interfere with the endocytosis of Egfr. Interestingly, in *tub-*

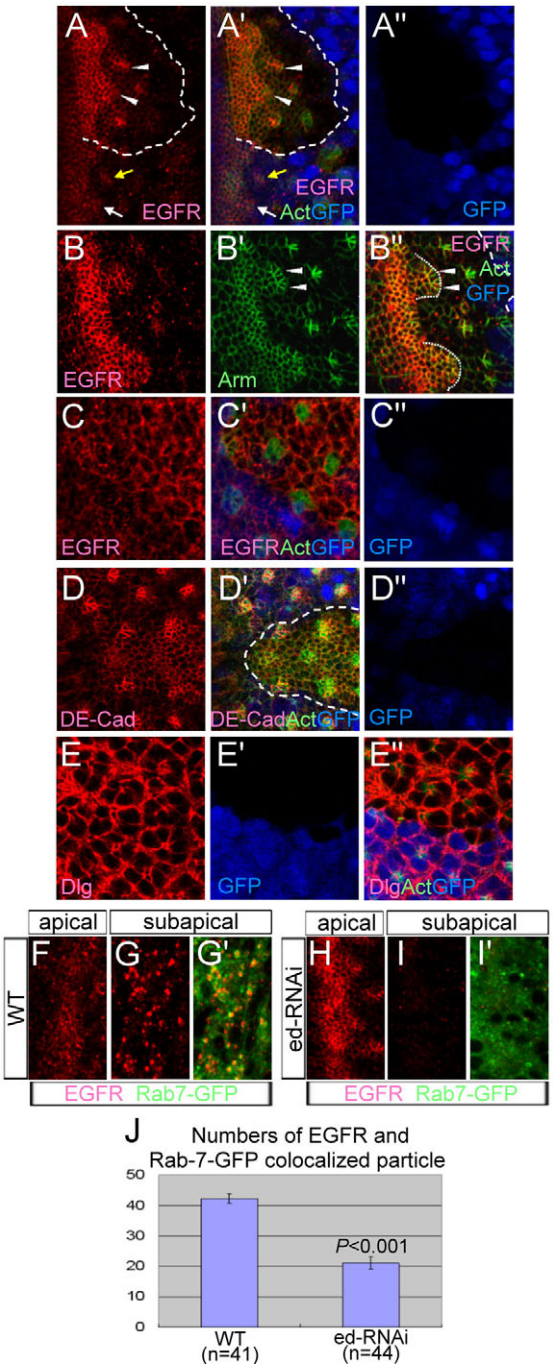

Fig. 5. Ed regulates the endocytosis of Egfr. (**A-A″**) ed^{1x5} mutant clone labeled for Egfr (red), GFP (blue) and actin (green). Arrowheads indicate the accumulation of higher levels of Egfr at rows 1 and 2. Dashed lines indicate the clonal border. (**B-B″**) High magnification of larger groups of arc cells in ed^{1x5} mutant clone labeled for Egfr (red), GFP (blue) and Arm (green). Arrowheads indicate the presence of two R8 cells in a larger group of arc cells (dotted lines) with upregulated Egfr. Dashed lines indicate the clonal border. (**C-C″**) Posterior ed^{1x5} mutant clone labeled for Egfr (red), GFP (blue) and actin (green). (**D-E″**) ed^{1x5} mutant clone labeled for DE-cad (red in D), Dlg (red in E), GFP (blue) and actin (green). Dashed lines indicate the clonal border. (**F-I'**) Colocalization of Egfr and Rab7-GFP. (F,H) Egfr (red) levels at the apical region of wild-type (F) and *tub-Gal80^{ts}-Gal4>ed-RNAi* (H) discs. (G,I) Colocalization of internalized Egfr (red) and Rab7-GFP (green) at subapical region of wild-type (G) and *tub-Gal80^{ts}-Gal4>ed-RNAi* (I) discs. (**J**) Quantitation of internalized Egfr and Rab7-GFP colocalized particles in wild-type and *tub-Gal80^{ts}-Gal4>ed-RNAi* discs. Bars indicate mean ± s.e.m.

Gal80^{ts}-Gal4>ed-RNAi discs, Egfr was upregulated at apical surfaces (compare Fig. 5F with 5H), but the numbers of internalized Egfr particles were significantly lower than in wild-type discs (compare Fig. 5G with 5I,J). Thus, Ed also regulates the endocytosis of Egfr.

Loss of *ed* leads to a rotation defect

Unlike DE-cad and Fmi, Ed is expressed mainly in ICs during PCP establishment. To explore whether *ed* might have an effect on PCP, we generated entirely ed^{1x5} mutant eyes in adults and observed PCP defects: randomized chirality (2%, n=145), R3/R3 symmetrical ommatidia (4%) and mostly misrotated ommatidia (94%) (Fig. 6A,B). As *ed* affects photoreceptor differentiation, here we only counted those ommatidia with a normal number of photoreceptors. The predominant misrotation phenotype detected in the *ed* mutant eyes, together with the observation that the initial localization of Fmi and Fz to the cell membranes of R3/R4 cells and the later asymmetric distribution to R4 cells were largely normal in *ed* mutant clones (Fig. 3A, arrowheads), suggest that the primary function of *ed* is to promote the later ommatidial rotation and that it has only minor effects on R3/R4 specification. Interestingly, similar to *DE-cad* (*shg*) clones, several wild-type clusters adjacent to *ed* mutant clones also showed misrotation (Fig. 6C; see Discussion).

It has been shown that *fmi* acts autonomously within ommatidia and is required in both R3 and R4 for planar polarity establishment (Das et al., 2002). Thus far we have demonstrated that loss of *ed* leads to accumulation of Fmi in ICs and to rotation defects (Fig. 3A, Fig. 6B). Moreover, fewer Fmi-upregulating ICs were required to border the apposed Fmi-expressing R3/R4 cells (Fig. 3C). Together, this prompted us to explore whether loss of *ed* might, via Fmi upregulation in ICs, affect ommatidial rotation. We generated small ectopic *fmi* clones in ICs to mimic the elevated Fmi that occurs within the *ed* mutant clones and then examined whether they affected adjacent cluster rotation. Similar to *ed* mutant clones, overexpressed Fmi recruited Fz/Dsh to the membrane of these cells (data not shown). Although overexpression of *fmi* in ICs did not affect the normal distribution of Fmi at the R3/R4 border of adjacent clusters (Fig. 6D,E, arrowheads), we observed misrotated ommatidia immediately adjacent to the *fmi*-overexpressing clones (Fig. 6D,E, arrowheads). Some *fmi* overexpression clones touched the R3/R4 pair of the misrotated ommatidia (Fig. 6E, arrowhead) and some clones touched the R8 cell of the misrotated ommatidia (Fig. 6D, arrowhead). Consistent with this, using *mδ0.5-lacZ* to mark R4 cells, we observed a misrotated ommatidium immediately adjacent to a small clone with as few as one or two *fmi*-overexpressing cells (Fig. 6F, arrowhead). This effect was specific, as small ectopic *DE-cad* (*shg*) clones in ICs did not lead to misrotation (Fig. 6G). However, these misrotated ommatidia occurred in only 45% of ommatidia (n=40), whereas the other 55% were mirror-image ommatidia (Fig. 6F, arrow), indicating a reversal of R3/R4 cell fate. Thus, overexpressed Fmi in the non-rotating ICs can affect both ommatidial rotation and R3/R4 specification of the adjacent clusters. This is different from the case of *ed* mutant clones, in which *ed* mainly promoted the later ommatidial rotation and had only minor effects on R3/R4 specification. As the levels of overexpressed Fmi in *fmi*-overexpressing clones were much higher than those observed in the *ed* mutant clones (compare Fig. 6D with Fig. 3A), this might explain this discrepancy.

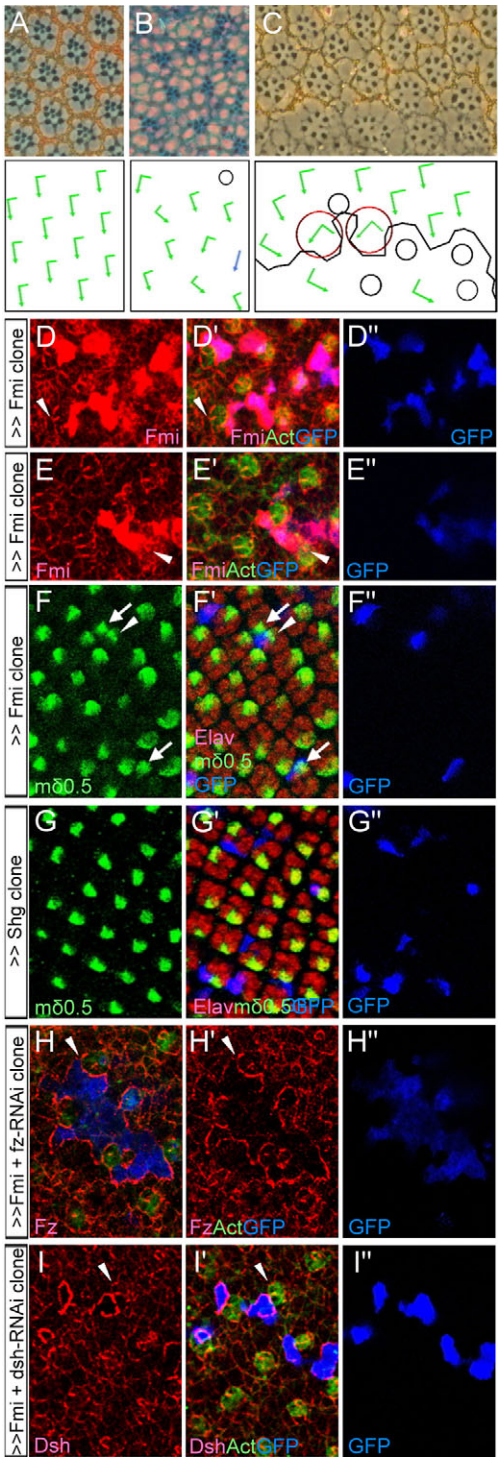

Fig. 6. Loss of *ed* leads to rotation defects. (**A**,**B**) Tangential sections of *Drosophila* adult eyes and (beneath) schematics illustrating dorsal chiral forms (green arrows). In wild-type eyes (A), all ommatidia are orientated at 90° to the equator, but eyes of entirely ed^{1x5} mutants (B) show misrotation, extra-photoreceptors (circle) and occasionally symmetrical ommatidia (blue arrow). (**C**) Sections of a mosaic ed^{1x5} eye region and the corresponding schematic (beneath). Black line indicates the clonal border. Clones were marked by the absence of pigment granules. Two wild-type ommatidia (red circles) show misrotation. (**D-E″**) *fmi* overexpression clones labeled for Fmi (red), GFP (blue) and actin (green). Arrowheads in D and E indicate the misrotated clusters that touch the *fmi* ectopic clone. (**F-F″**) *fmi* overexpression clones labeled for *mδ0.5-lacZ* (green), Elav (red) and GFP (blue). Arrowhead and arrow indicate the misrotated and mirror-image cluster, respectively. (**G-G″**) *shg* overexpression clones labeled for *mδ0.5-lacZ* (green), Elav (red) and GFP (blue). (**H-H″**) *fmi+fz-RNAi* overexpression clones labeled for Fz (red), GFP (blue) and actin (green). Arrowhead indicates the misrotated clusters that touch the clone. (**I-I″**) *fmi+dsh-RNAi* overexpression clones labeled for Dsh (red), GFP (blue) and actin (green). Arrowhead indicates the misrotated clusters that touch the clone.

Fmi is a homophilic CAM, which we confirmed here by generating *fmi-RNAi* clones. We found that the enrichment of Fmi at the R3/R4 border was eliminated when an *fmi-RNAi* R3 cell contacted a wild-type R4 cell (data not shown). Thus, one simple scenario to explain the predominate misrotated ommatidia phenotype of the *ed* mutant clone is that the moderately elevated Fmi expressed by ICs might interact with Fmi on the surface of a rotating cluster to interfere with later cluster rotation. Fmi was enriched on R3, R4 and R8 (Fig. 1). If the homophilic binding between Fmi on the cells of the rotating cluster and the non-rotating ICs is the driving force for the misrotation, we would expect that the Fmi-associated Fz/Dsh should be dispensable in the ICs for the misrotation of clusters adjacent to the *ed* mutant tissues. To test this, we generated ectopic clones overexpressing both *fmi* and *fz-RNAi* to deplete Fz within the *fmi*-overexpressing clones. Interestingly, Fz (and the associated Dsh) was largely depleted in the *fmi*-overexpressing clone but instead accumulated at the clone border (Fig. 6H). As Fmi is a homophilic CAM, this result indicates that the accumulated Fz was recruited by Fmi on the wild-type cells surrounding the *fmi,fz-RNAi* clones. Nevertheless, we still observed that *fmi,fz-RNAi* clones, similar to *fmi* clones, touched the R3/R4 pair of the misrotated ommatidia (Fig. 6H). Moreover, using *mδ0.5-lacZ* to mark R4 cells, we also observed rotation defects of ommatidial clusters outside the *fmi,fz-RNAi* clones (data not shown). Similar results were obtained when we generated *fmi,dsh-RNAi* clones to deplete *dsh* within the *fmi*-overexpressing clones (Fig. 6I). Altogether, our results suggest that elevated Fmi on the non-rotating ICs, possibly via homophilic binding, interferes with the correct rotation of the adjacent clusters. This is consistent with the idea that upregulation of Fmi in the ICs contributes to the rotation defects associated with the loss of *ed*.

DISCUSSION

In this study, we found that Ed interacts with AP-2 and promotes Fmi internalization via a clathrin-dependent pathway in ICs. Moreover, loss of *ed* leads to accumulation of Fmi (and of several receptors/CAMs of AJs) on the membrane of these non-rotating ICs. This, together with the observation that overexpression of *fmi* in the non-rotating ICs is sufficient to cause photoreceptor misrotation, led us to propose an Ed-mediated co-endocytosis model to explain the rotation defects associated with the *ed* mutant tissue. Thus, the homophilic CAMs, Ed and Fmi, play crucial roles in ICs to allow coordinated rotation of ommatidial clusters.

Ed-mediated co-endocytosis

We have demonstrated here that Ed specifically regulates Fmi endocytosis in ICs. Although Fmi was previously shown to be endocytosed in the photoreceptor cluster (Rawls and Wolff, 2003), we argue that Fmi levels in the rotating photoreceptor clusters are regulated by an Ed-independent mechanism. First, Fmi levels in the photoreceptor clusters are not affected in the *ed* mutant clones. Second, the Fmi distribution pattern in R3/R4 is largely unchanged

even when *Ed-GFP* is overexpressed in photoreceptors by *Elav-Gal4* to mimic the *ed*-expressing ICs (J.-C.H., unpublished). We have also demonstrated that Ed levels in ICs, but not in photoreceptor clusters, are regulated via an AP-2-dependent endocytic pathway. It remains unknown how Ed is downregulated in the photoreceptor cluster. Egfr signaling has been proposed to regulate the morphological and adhesive changes of cells within the photoreceptor cluster (Brown et al., 2006), and it is possible that Egfr signaling directly or indirectly downregulates the Ed levels in R8/R2/R5 and later in R3/R4.

Interestingly, *ed* affects the levels of Fmi, DE-cad and Egfr, but not of Dlg. Therefore, Ed seems to only affect receptors/CAMs at AJs. One intriguing possibility is that Ed, via its interaction with AP-2, triggers the co-endocytosis of most, if not all, of the receptor/CAM at AJs. Although Ed has been shown to associate with Egfr (Spencer and Cagan, 2003), there is currently no evidence that Ed interacts directly with Fmi. Thus, Ed might undergo co-endocytosis either directly or indirectly. Although Ed contains five putative protein-sorting motifs, it is not the only molecule with a protein-sorting motif: Egfr, for example, also contains the YXXΦ signal. It is possible that different receptors/CAMs might cooperate, via their interaction with AP-2 or other adaptors, to promote the co-endocytosis of other receptors/CAMs.

Because Ed facilitates the endocytosis of many receptors/CAMs of AJs, although to different extents, we would expect multiple functions of *ed* in the eye disc. Indeed, *ed* plays crucial roles in PCP (this study) and in Egfr signaling (Bai et al., 2001; Rawlins et al., 2003a; Spencer and Cagan, 2003) during eye development. It was previously shown that loss of *ed* leads to sustained MAPK (Rolled – FlyBase) activation only in cells of the proneural clusters and over several rows (Spencer and Cagan, 2003). This is consistent with our observation that Egfr was upregulated in an enlarged group of arc cells that contains two R8 photoreceptors as well as in cells of developing ommatidia up to two rows posterior to the MF. Thus, it is plausible that Ed was co-endocytosed with Egfr in the proneural clusters to downregulate Egfr activity within these cells and thus ensure that only one R8 is selected from the two to three R8 cell-equivalent group. When *ed* is absent, Egfr cannot be internalized efficiently and therefore persists on the membrane to cause sustained MAPK activation and multiple R8 selection. Although the level of Egfr is also upregulated in cells more posterior to the MF, these levels might not be high enough to cause sustained MAPK activation. In the wing disc, Ed also facilitates Notch signaling to promote mesothorax bristle patterning (Ahmed et al., 2003; Escudero et al., 2003; Rawlins et al., 2003b). In fact, Ed colocalizes with Notch/Delta in Hrs-containing early endosomes (Escudero et al., 2003; Rawlins et al., 2003b). However, it remains unclear whether the endocytosis of Ed plays any role in facilitating Notch signaling in the wing discs.

Ed and PCP

It has been shown that each photoreceptor cluster, as a group, moves independently of the adjacent ICs (Fiehler and Wolff, 2007). Most rotation-specific genes identified thus far have been proposed to function mainly in the rotating clusters to modulate rotation. Here, we provide evidence that Ed plays crucial roles in the ICs to modulate ommatidial rotation. We propose that Ed, via co-endocytosis, reduces the level of Fmi on the non-rotating ICs to prevent homotypic interactions with the enriched Fmi on the rotating cluster. This allows free and coordinated rotation of photoreceptor clusters, a process regulated by effectors such as Zipper and Nemo (Fiehler and Wolff, 2007; Fiehler and Wolff, 2008). We reason that in the absence of *ed*, as seen in *ed* mutant clones, the upregulated Fmi on the non-rotating ICs might affect the free rotation of ommatidial clusters not only within the *ed* clone, but also in the adjacent wild-type clusters abutting the *ed* clones. This might contribute, at least in part, to the non-autonomous effect of *ed* on ommatidial rotation (Fig. 6C). The dynamic and differential expression of Ed (and of its paralog Friend of Echinoid) in the rotating clusters and non-rotating ICs has also been proposed to modulate ommatidial rotation (Fetting et al., 2009). Thus, differential expression of Ed, Fmi, DE-cad and Friend of Echinoid in the rotating clusters and non-rotating ICs prevents the homotypic interaction of these four CAMs to allow free rotation of photoreceptor clusters. The largely complementary expression pattern between Ed and DE-cad/Arm in a photoreceptor cluster is similar to that observed during the generation of *ed* mutant clones in the wing discs, where Ed-non-expressing cells accumulate high levels of DE-cad/Arm and sort out from the surrounding Ed-expressing cells (Wei et al., 2005). Thus, cell sorting-like behavior of a photoreceptor cluster, mediated by differential expression of Ed and DE-cad/Arm, might help photoreceptors in the cluster to rotate as a group.

Fetting et al. recently showed that *ed* genetically interacts with Egfr pathway members, and proposed that *ed*, via inhibiting Egfr signaling in the photoreceptors, regulates ommatidial rotation (Fetting et al., 2009). However, we demonstrated that, after row 2, Ed facilitates the endocytosis of Egfr only in the non-rotating ICs, but not in the photoreceptor clusters (Fig. 5C). Thus, if Ed indeed inhibits Egfr signaling in the photoreceptors as suggested, it probably employs mechanisms other than to reduce the levels of Egfr on the photoreceptors. It is currently unknown whether the effect of Ed on Egfr levels in ICs plays any role in the modulation of ommatidial rotation. Moreover, we found that in the absence of *ed*, not only Fmi, Fz and Dsh (the R3-specific PCP proteins), but also Strabismus (Van Gogh – FlyBase) and its associated Prickle (the R4-specific PCP proteins) were all upregulated in ICs, but their enrichment at R3/R4 borders in the photoreceptor cluster was largely unaffected (Fig. 3D) (J.-C.H., unpublished). As *ed* affects the levels of all the core PCP proteins tested in ICs, it remains unclear how *ed* only interacts genetically with the R3-specific PCP genes to modulate the degree of ommatidial rotation (Fetting et al., 2009). Finally, *ed* also weakly affects the initial R3/R4 specification, as a small proportion of *ed* mutant cells also show randomized chirality and symmetrical ommatidia. It is possible that *ed* might exert this effect through mechanisms other than the promotion of Fmi endocytosis. Alternatively, as overexpression of Fmi in the non-rotating ICs (generated by *fmi*-overexpressing clones) can affect both ommatidial rotation and reversal of R3/R4 cell fate of the adjacent clusters, it is possible that the Fmi upregulation in the ICs (generated by *ed* mutant clones) might also affect, to some extent, the asymmetric distribution of Fmi in R3/R4 and, thereby, the R3/R4 specification of the adjacent clusters.

Acknowledgements

We thank D. Strutt, T. Uemura, H. Bellen, L.-M. Pai, the Developmental Studies Hybridoma Bank (DSHB) and the Vienna *Drosophila* RNAi Center (VDRC) for providing reagents and stocks; and D. Strutt also for comments on the manuscript. Grants from the National Science Council, Taiwan, to J.-C.H. are acknowledged.

Competing interests statement

The authors declare no competing financial interests.

Supplementary material

Supplementary material for this article is available at
http://dev.biologists.org/lookup/suppl/doi:10.1242/dev.040238/-/DC1

References

Adler, P. N., Charlton, J. and Liu, J. (1998). Mutations in the cadherin superfamily member gene *dachsous* cause a tissue polarity phenotype by altering Frizzled signaling. *Development* **125**, 959-968.

Ahmed, A., Chandra, S., Magarinos, M. and Vaessin, H. (2003). Echinoid mutants exhibit neurogenic phenotypes and show synergistic interactions with the Notch signaling pathway. *Development* **130**, 6295-6304.

Axelrod, J. D., Miller, J. R., Shulman, J. M., Moon, R. T. and Perrimon, N. (1998). Differential recruitment of Dishevelled provides signaling specificity in the planar cell polarity and Wingless signaling pathways. *Genes Dev.* **12**, 2610-2622.

Bai, J., Chiu, W., Wang, J., Tzeng, T., Perrimon, N. and Hsu, J. (2001). The cell adhesion molecule Echinoid defines a new pathway that antagonizes the Drosophila EGF receptor signaling pathway. *Development* **128**, 591-601.

Bastock, R. and Strutt, D. (2007). The planar polarity pathway promotes coordinated cell migration during Drosophila oogenesis. *Development* **134**, 3055-3064.

Brown, K. E. and Freeman, M. (2003). Egfr signalling defines a protective function for ommatidial orientation in the Drosophila eye. *Development* **130**, 5401-5412.

Brown, K. E., Baonza, A. and Freeman, M. (2006). Epithelial cell adhesion in the developing Drosophila retina is regulated by Atonal and the EGF receptor pathway. *Dev. Biol.* **300**, 710-721.

Chae, J., Kim, M. J., Goo, J. H., Collier, S., Gubb, D., Charlton, J., Adler, P. N. and Park, W. J. (1999). The Drosophila tissue polarity gene *starry night* encodes a member of the protocadherin family. *Development* **126**, 5421-5429.

Chang, W. L., Liou, W., Pen, H. C., Chou, H. Y., Chang, Y. W., Li, W. H., Chiang, W. and Pai, L. M. (2008). The gradient of Gurken, a long-range morphogen, is directly regulated by Cbl-mediated endocytosis. *Development* **135**, 1923-1933.

Chen, M. S., Obar, R. A., Schroeder, C. C., Austin, T. W., Poodry, C. A., Wadsworth, S. C. and Vallee, R. B. (1991). Multiple forms of dynamin are encoded by *shibire*, a Drosophila gene involved in endocytosis. *Nature* **351**, 583-586.

Cooper, M. T. and Bray, S. J. (1999). Frizzled regulation of Notch signalling polarizes cell fate in the Drosophila eye. *Nature* **397**, 526-530.

Das, G., Reynolds-Kenneally, J. and Mlodzik, M. (2002). The atypical cadherin Flamingo links Frizzled and Notch signaling in planar polarity establishment in the Drosophila eye. *Dev. Cell* **2**, 655-666.

Entchev, E. V., Schwabedissen, A. and Gonzalez-Gaitan, M. (2000). Gradient formation of the TGF-beta homolog Dpp. *Cell* **103**, 981-991.

Escudero, L. M., Wei, S. Y., Chiu, W. H., Modolell, J. and Hsu, J. C. (2003). Echinoid synergizes with the Notch signaling pathway in Drosophila mesothorax bristle patterning. *Development* **130**, 6305-6316.

Fanto, M. and Mlodzik, M. (1999). Asymmetric Notch activation specifies photoreceptors R3 and R4 and planar polarity in the Drosophila eye. *Nature* **397**, 523-526.

Fetting, J. L., Spencer, S. A. and Wolff, T. (2009). The cell adhesion molecules Echinoid and Friend of Echinoid coordinate cell adhesion and cell signaling to regulate the fidelity of ommatidial rotation in the Drosophila eye. *Development* **136**, 3323-3333.

Fiehler, R. W. and Wolff, T. (2007). Drosophila myosin II, Zipper, is essential for ommatidial rotation. *Dev. Biol.* **310**, 348-362.

Fiehler, R. W. and Wolff, T. (2008). Nemo is required in a subset of photoreceptors to regulate the speed of ommatidial rotation. *Dev. Biol.* **313**, 533-544.

Freeman, M. (1996). Reiterative use of the EGF receptor triggers differentiation of all cell types in the Drosophila eye. *Cell* **87**, 651-660.

Gaengel, K. and Mlodzik, M. (2003). Egfr signaling regulates ommatidial rotation and cell motility in the Drosophila eye via MAPK/Pnt signaling and the Ras effector Canoe/AF6. *Development* **130**, 5413-5423.

Hacohen, N., Kramer, S., Sutherland, D., Hiromi, Y. and Krasnow, M. A. (1998). *sprouty* encodes a novel antagonist of FGF signaling that patterns apical branching of the Drosophila airways. *Cell* **92**, 253-263.

Hayashi, T. and Carthew, R. W. (2004). Surface mechanics mediate pattern formation in the developing retina. *Nature* **431**, 647-652.

Hicke, L. and Dunn, R. (2003). Regulation of membrane protein transport by ubiquitin and ubiquitin-binding proteins. *Annu. Rev. Cell Dev. Biol.* **19**, 141-172.

Islam, R., Wei, S. Y., Chiu, W. H., Hortsch, M. and Hsu, J. C. (2003). Neuroglian activates Echinoid to antagonize the Drosophila EGF receptor signaling pathway. *Development* **130**, 2051-2059.

Ito, K., Awano, W., Suzuki, K., Hiromi, Y. and Yamamoto, D. (1997). The Drosophila mushroom body is a quadruple structure of clonal units each of which contains a virtually identical set of neurones and glial cells. *Development* **124**, 761-771.

Kimura, H., Usui, T., Tsubouchi, A. and Uemura, T. (2006). Potential dual molecular interaction of the Drosophila 7-pass transmembrane cadherin Flamingo in dendritic morphogenesis. *J. Cell Sci.* **119**, 1118-1129.

Klein, T. J. and Mlodzik, M. (2005). Planar cell polarization: an emerging model points in the right direction. *Annu. Rev. Cell Dev. Biol.* **21**, 155-176.

Lin, H. P., Chen, H. M., Wei, S. Y., Chen, L. Y., Chang, L. H., Sun, Y. J., Huang, S. Y. and Hsu, J. C. (2007). Cell adhesion molecule Echinoid associates with unconventional myosin VI/Jaguar motor to regulate cell morphology during dorsal closure in Drosophila. *Dev. Biol.* **311**, 423-433.

Littleton, J. T. and Bellen, H. J. (1994). Genetic and phenotypic analysis of thirteen essential genes in cytological interval 22F1-2; 23B1-2 reveals novel genes required for neural development in Drosophila. *Genetics* **138**, 111-123.

Mahoney, P. A., Weber, U., Onofrechuk, P., Biessmann, H., Bryant, P. J. and Goodman, C. S. (1991). The *fat* tumor suppressor gene in Drosophila encodes a novel member of the cadherin gene superfamily. *Cell* **67**, 853-868.

Mirkovic, I. and Mlodzik, M. (2006). Cooperative activities of drosophila DE-cadherin and DN-cadherin regulate the cell motility process of ommatidial rotation. *Development* **133**, 3283-3293.

Mlodzik, M. (2002). Planar cell polarization: do the same mechanisms regulate Drosophila tissue polarity and vertebrate gastrulation? *Trends Genet.* **18**, 564-571.

Newsome, T. P., Asling, B. and Dickson, B. J. (2000). Analysis of Drosophila photoreceptor axon guidance in eye-specific mosaics. *Development* **127**, 851-860.

Oda, H. and Tsukita, S. (2001). Real-time imaging of cell-cell adherens junctions reveals that Drosophila mesoderm invagination begins with two phases of apical constriction of cells. *J. Cell Sci.* **114**, 493-501.

Rawlins, E. L., White, N. M. and Jarman, A. P. (2003a). Echinoid limits R8 photoreceptor specification by inhibiting inappropriate EGF receptor signalling within R8 equivalence groups. *Development* **130**, 3715-3724.

Rawlins, E. L., Lovegrove, B. and Jarman, A. P. (2003b). Echinoid facilitates Notch pathway signalling during Drosophila neurogenesis through functional interaction with Delta. *Development* **130**, 6475-6484.

Rawls, A. S. and Wolff, T. (2003). Strabismus requires Flamingo and Prickle function to regulate tissue polarity in the Drosophila eye. *Development* **130**, 1877-1887.

Robinson, M. S. (2004). Adaptable adaptors for coated vesicles. *Trends Cell Biol.* **14**, 167-174.

Sanson, B., White, P. and Vincent, J. P. (1996). Uncoupling cadherin-based adhesion from wingless signalling in Drosophila. *Nature* **383**, 627-630.

Seto, E. S., Bellen, H. J. and Lloyd, T. E. (2002). When cell biology meets development: endocytic regulation of signaling pathways. *Genes Dev.* **16**, 1314-1336.

Spencer, S. A. and Cagan, R. L. (2003). Echinoid is essential for regulation of Egfr signaling and R8 formation during Drosophila eye development. *Development* **130**, 3725-3733.

Stowers, R. S. and Schwarz, T. L. (1999). A genetic method for generating Drosophila eyes composed exclusively of mitotic clones of a single genotype. *Genetics* **152**, 1631-1639.

Strutt, D. (2003). Frizzled signalling and cell polarisation in Drosophila and vertebrates. *Development* **130**, 4501-4513.

Strutt, D., Johnson, R., Cooper, K. and Bray, S. (2002). Asymmetric localization of Frizzled and the determination of Notch-dependent cell fate in the Drosophila eye. *Curr. Biol.* **12**, 813-824.

Strutt, H. and Strutt, D. (2003). EGF signaling and ommatidial rotation in the Drosophila eye. *Curr. Biol.* **13**, 1451-1457.

Strutt, H. and Strutt, D. (2008). Differential stability of Flamingo protein complexes underlies the establishment of planar polarity. *Curr. Biol.* **18**, 1555-1564.

Strutt, H., Price, M. A. and Strutt, D. (2006). Planar polarity is positively regulated by casein kinase Iepsilon in Drosophila. *Curr. Biol.* **16**, 1329-1336.

Tomlinson, A. and Struhl, G. (1999). Decoding vectorial information from a gradient: sequential roles of the receptors Frizzled and Notch in establishing planar polarity in the Drosophila eye. *Development* **126**, 5725-5738.

Usui, T., Shima, Y., Shimada, Y., Hirano, S., Burgess, R. W., Schwarz, T. L., Takeichi, M. and Uemura, T. (1999). Flamingo, a seven-pass transmembrane cadherin, regulates planar cell polarity under the control of Frizzled. *Cell* **98**, 585-595.

van der Bliek, A. M. and Meyerowitz, E. M. (1991). Dynamin-like protein encoded by the Drosophila *shibire* gene associated with vesicular traffic. *Nature* **351**, 411-414.

Waddell, S., Armstrong, J. D., Kitamoto, T., Kaiser, K. and Quinn, W. G. (2000). The *amnesiac* gene product is expressed in two neurons in the Drosophila brain that are critical for memory. *Cell* **103**, 805-813.

Wei, S. Y., Escudero, L. M., Yu, F., Chang, L. H., Chen, L. Y., Ho, Y. H., Lin, C. M., Chou, C. S., Chia, W., Modolell, J. et al. (2005). Echinoid is a component of adherens junctions that cooperates with DE-cadherin to mediate cell adhesion. *Dev. Cell* **8**, 493-504.

Wolff, T. and Ready, D. F. (1993). Pattern formation in Drosophila retina. In *The Development of Drosophila melanogaster* (ed. M. Bate and A. Martinez-Arias), pp. 1277-1325. Cold Spring Harbor, New York: Cold Spring Harbor Laboratory Press.

Wucherpfennig, T., Wilsch-Brauninger, M. and Gonzalez-Gaitan, M. (2003). Role of Drosophila Rab5 during endosomal trafficking at the synapse and evoked neurotransmitter release. *J. Cell Biol.* **161**, 609-624.

Yang, C. H., Axelrod, J. D. and Simon, M. A. (2002). Regulation of Frizzled by fat-like cadherins during planar polarity signaling in the Drosophila compound eye. *Cell* **108**, 675-688.

Zheng, L., Zhang, J. and Carthew, R. W. (1995). frizzled regulates mirror-symmetric pattern formation in the Drosophila eye. *Development* **121**, 3045-3055.